VPS VIBRATIONS IN PHYSICAL SYSTEMS

DOI: 10.21008/j.0860-6897.2022.1.04
Vibrations in Physical Systems, 2022, 33(1), 2022104

Numerical Investigation of Noise Generated by an Axial Fan Installed in a Pipeline

Dawid ROMIK

AGH University of Science and Technology, Faculty of Mechanical Engineering and Robotics, Al. Mickiewicza 30, 30-059 Krakow, Poland

Corresponding author: Dawid ROMIK, email: dromik@agh.edu.pl

Abstract The article presents the results of numerical calculations of noise generated by an axial fan installed in a ventilation duct with a circular cross-section. The research takes into account the installation of the axial fan due to the distance of the rotor from the curvature of the pipeline. The uRANS turbulent flow modeling methods were used in the calculations. The uRANS stands for the Navier-Stokes equation with Reynolds averaging in the version that takes into account the non-stationarity of the flow. The purpose of the work is to determine the sound power in the vicinity of the sound source. The decisive parameters affecting the noise emitted will be the length of the installation in front of and behind the rotor. The propagation of acoustic disturbances in the far field was modeled using the aeroacoustic analogy of Ffowcs-Williams and Hawkings. Based on the calculations, the directional characteristics of the sound source were determined.

Keywords: noise, numerical methods, CFD, aeroacoustics, turbomachinery.

1. Introduction

Fans usually operate under very turbulent influx conditionsdue to e.g. their installation in a pipeline and coolers influence etc. This causes very unstable aerodynamic forces on the rotor blades which in turn cause excessive sound radiation. Aeroacoustic-art computational methods allow more reliable prediction of the generated noise. Typically, they require detailed knowledge of the transient flow field obtained by simulation by computational fluid dynamics.

The most accurate method, Direct Numerical Simulation (DNS), solves the Navier Stokes equation without any simplification and predicts unstable flow and the corresponding acoustic field. Unfortunately, direct numerical simulation is not feasible for complex geometry such as a fan due to enormous computational costs. Finding a non-stationary flow field with less effort requires modeling at least some of the turbulent fluctuations. Currently, two different methods are used to reduce computational costs. The first is time averaging known as Unsteady Reynolds Averaged Navier Stokes Simulation (uRANS), the second is filtering of the full Navier Stokes equations called Large Eddy Simulation (LES). In the case of uRANS computational cost reduction it is huge, but the compromise is a high degree of approximation. All random turbulent fluctuations are modeled, therefore only tonal sources of axial fan sound can be predicted. This article aims to investigate the noise generated by the axial fan installed in a pipe of circular cross section by uRANS method. Studies using these methods have been presented, among others, in [1-4].

2. Research object

The object of the research is an axial fan with a diameter of 220 mm, rotating at a rotational speed of 3000 revolutions per minute built in a pipeline with a circular cross-section with a diameter of 230 mm (see Fig. 1-2). For the assumed rotational speed, the fan achieves efficiency of approx. 750 m^3/s.

2.1. Geometric model

Two characteristic zones can be distinguished in the model: the rotating zone, in which the rotor is located, and the stationary one, i.e. a curved pipeline. The geometric model does not include the fan fasteners inside the pipeline. To simplify the model, steering systems and elements straightening air streams were also omitted. In the geometric model, the lengths of the channel in front of and behind the rotor are marked.

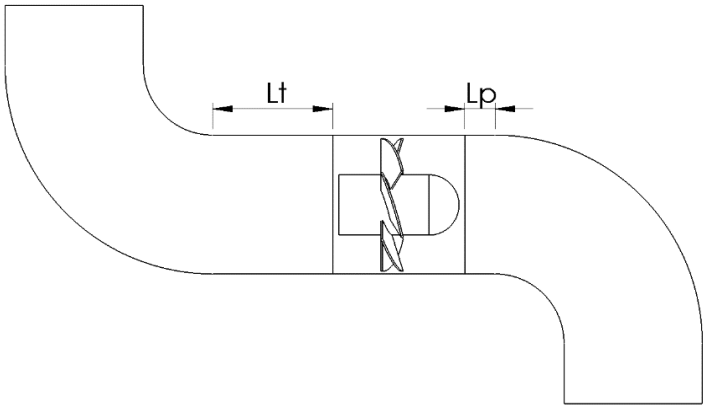

Figure 1. Axial fan installed in the pipeline.

(a) (b)

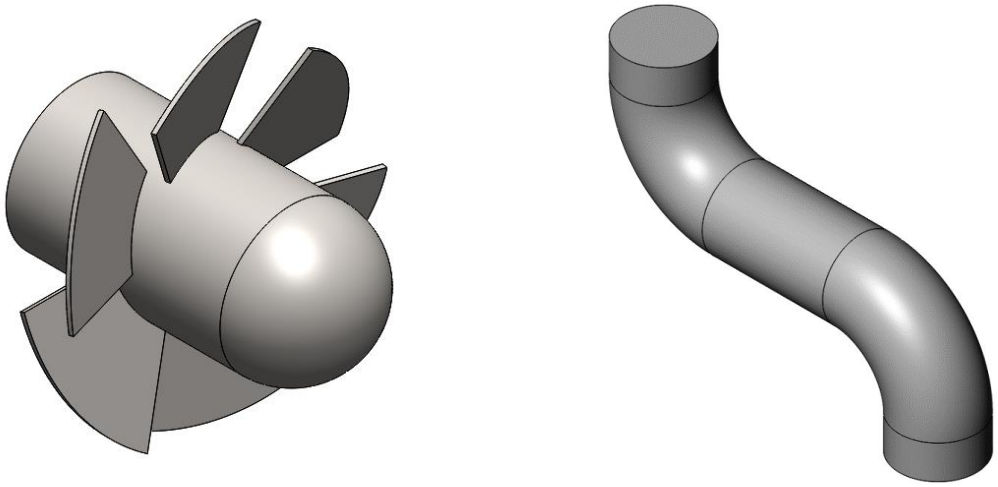

Figure 2. Geometric model: a) rotor, b) pipeline.

3. Numerical calculations

Numerical calculations were made in the Ansys Fluent software with the use of high-power computers located in the Academic Computer Centre Cyfronet AGH

3.1. Numerical model

The model consists of two zones: inlet and outlet, which consists of a stationary zone, and a rotating zone containing the rotor. To set the rotor in motion, the sliding mesh method was used, which means that at each time step there is an angular shift of the rotational zone. The model was divided into finite volumes. The generated mesh consisted of 1 017 564 nodes, of which approx. 67% was in the rotating zone (see Fig. 3).

(a) (b)

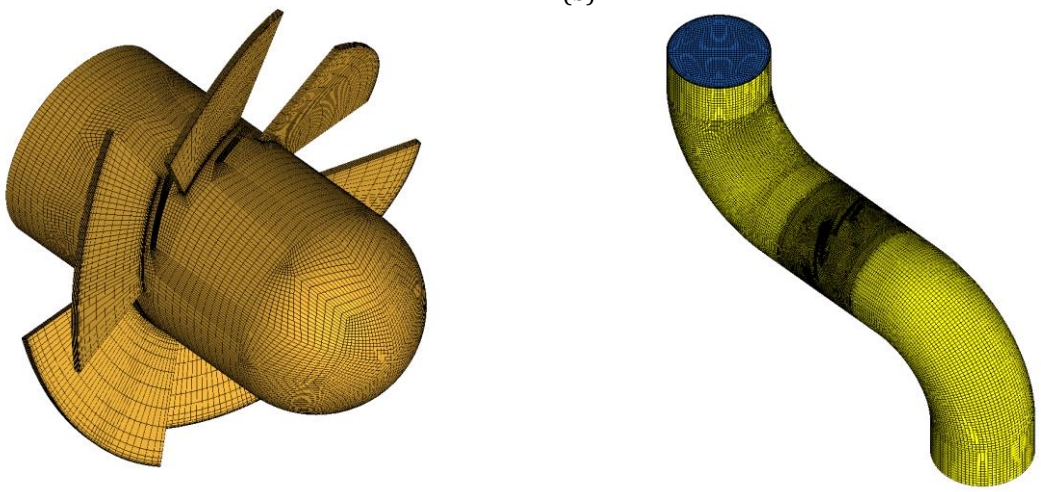

Figure 3. Numerical model: a) rotor computing grid, b) pipeline computing grid.

Increasing the number of cells did not cause significant changes in velocity and pressure distributions in the model. The dimensionless y^+ coefficient characterizing the ability of the mesh to model the boundary layer was in the range of 1-2. The boundary condition *Wall* was applied to the rotor surfaces and the walls of the pipeline, preventing the air flow through the indicated surfaces. At the inlet of the pipeline, the *Pressure Inlet* condition was imposed and the *Pressure Outlet* condition at the outlet, corresponding to the atmospheric pressure. The rotating zone was set into motion with a rotational speed of 3000 rpm. The time step $t = 5.5 \cdot 10^{-5}$corresponds to 1° of the rotor rotation. An incompressible fluid model was used. The model described by the Reynolds Averaged Navier Stokes continuity equations was adopted for the calculations. Menter's turbulent model k-ω SST was used to close the mathematical model [5, 6]. Since the acceleration of the rotor is not taken into consideration, it was decided primarily to speed up the calculation, by simulating the steady state, and after reaching the convergence of the results of the calculation start time varying at a constant speed. For the assumed boundary conditions, the flow was established after about 10 rotations of the rotor.

3.2. Acoustic model

A model based on the analogy of Ffowcs Williams - Hawkings (FW-H) [7] was used to determine the sound pressure level. This model takes the general form of the Lighthill acoustic analogy [8] and can predict the sound generated by equivalent acoustic sources such as monopoles, dipoles and quadrupoles. The Ansys Fluent program adopts an equation in which the sound pressure and the acoustic signal at designated locations are calculated by finding several integrals over the surface. The FW-H equation is a non-uniform wave equation that can be determined by coupling the continuity equations and the Navier-Stokes equations. It can be written as

$$\begin{aligned} &\frac{1}{a_0^2}\frac{\partial^2 p'}{\partial t^2} - \nabla^2 p' = \frac{\partial^2}{\partial x_i \partial x_j}\{T_{ij}H(f)\} \\ &-\frac{\partial}{\partial x_i}\{|P_{ij}n_j + \rho u_i(u_n - v_n)|\delta(f)\} \\ &+\frac{\partial}{\partial t}\{|\rho_0 v_n + \rho(u_n - v_n)|\delta(f)\} \end{aligned} \tag{1}$$

where: u_i – fluid velocity component in the x_i direction, u_n– fluid velocity component normal to the surface f=0, v_i – surface velocity components in the x_i direction, v_n – surface velocity component normal to the surface, $\delta(f)$ – Dirac delta function, $H(f)$ – Heaviside function, p' – sound pressure at the far field ($p' - p0$), n_i – normal vector pointing toward the exterior region ($f > 0$), a_0 – far-field sound speed, T_{ij} – Lighthill stress tensor, P_{ij}– compressive stress tensor.

The solution to equation (1) is obtained by using Green's function $(\delta(g)/4\pi r)$. The complete solution is to calculate surface integrals and volume integrals, the first of which represent monopoly, dipole, and

semi-quadrupole acoustic sources, and the second represent quadrupole sources in the region beyond the source surface. The proportion of volume integrals becomes small when the flow is low subsonic and the source surface covers the source region. In the ANSYS FLUENT program, the volume integrals are ignored, then [6]:

$$p'(x,t) = p'_T(x,t)p'_L(x,t), \tag{2}$$

$$4\pi p'_T(x,t) = \int_{f=0}\left[\frac{\rho_0(\dot{U}_n + \dot{U}_n)}{r(1-M_r)^2}\right]dS + \int_{f=0}\left[\frac{\rho_0 U_n r\dot{M}_r + a_0(M_r - M^2)}{r^2(1-M_r)^3}\right]dS, \tag{3}$$

$$4\pi p'_L(x,t) = \frac{1}{a_0}\int_{f=0}\left[\frac{\dot{L}_r}{r(1-M_r)^2}\right]dS + \int_{f=0}\left[\frac{L_r - L_M}{r^2(1-M_r)^2}\right]dS + \frac{1}{a_0}\int_{f=0}\left[\frac{L_r r\dot{M}_r + a_0(M_r - M^2)}{r^2(1-M_r)^3}\right]dS, \tag{4}$$

where

$$U_i = v_i + \frac{\rho}{\rho_0}(u_i - v_i), \tag{5}$$

$$L_i = P_{ij}n_j + \rho u_i(u_n - v_n).$$

Considering the time t and the distance to the observer r, the integral of the above equation is computed at the time given by equation

$$U_i = v_i + \frac{\rho}{\rho_0}(u_i - v_i) \tag{6}$$

$$L_i = P_{ij}n_j + \rho u_i(u_n - v_n) \tag{7}$$

where n, r – unit vectors of radiation and wall normals, M – Mach number of the velocity component of the surface source along the direction of the radiation vector.

4. Results and conclusions

The criterion for determining the flow was the torque on the rotor, which stabilized after approx. 3500 time steps. The contours of the air velocity passing through the fan in the cross-section of the OX axis are shown in the figure 4. In addition to the sound pressure was also calculated operating parameters such as fan torque on the rotor, the accumulation of total pressure, mechanical power output, and efficiency. The results are presented and in the graph (see Fig. 5) and Table 1.

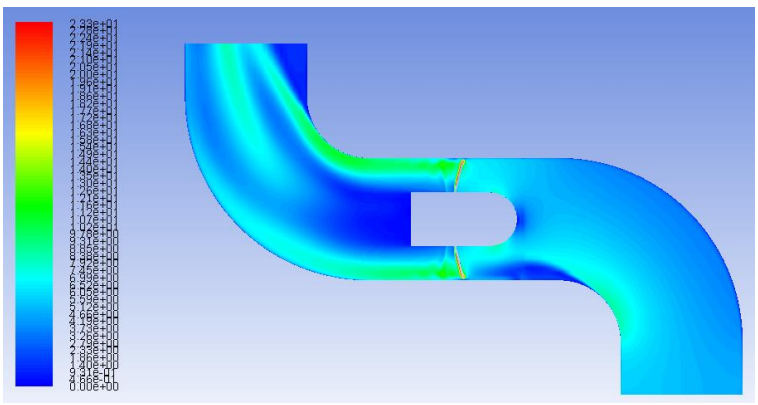

Figure 4. Velocity contours.

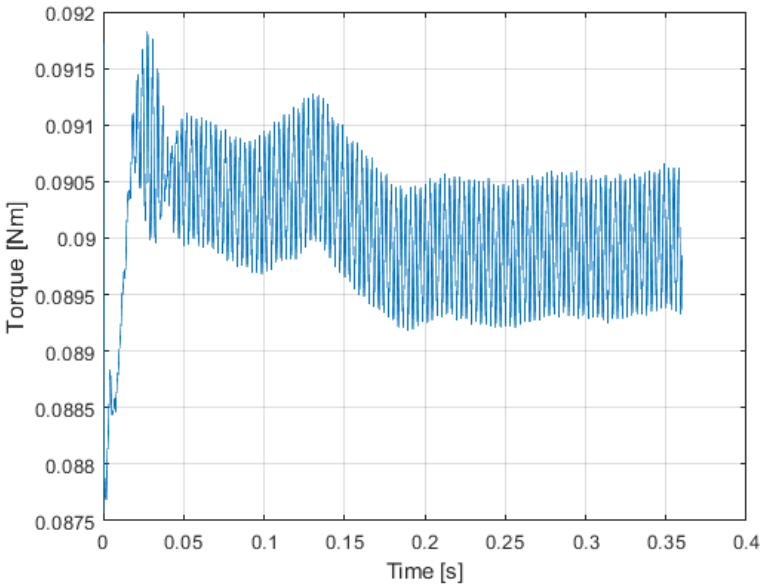

Figure 5. Rotor torque.

Table 1. Calculated operating parameters.

Quantity	Symbol	Unit	Value
Rotor torque	M	Nm	0.090
Total pressure gain	Δp	Pa	30.063
Volume flow rate	$\dot{V}$	m^3/s	759.903
Useful power	N_u	W	8.282
Mechanical power	N_m	W	28.302
Efficiency	η	–	0.293
RMS sound pressure	p_{RMS}	Pa	0.0085
Sound pressure level	L_p	dB	52.55

The acoustic pressure calculated during the simulation was recorded on receivers distributed evenly within a radius of 3 m from the source. A total of 510 receivers were generated. In each of them, an acoustic signal was recorded with the number of samples equal to 7200, from which the sound pressure level was calculated. The surfaces of the fan and the pipeline were assumed as the source of sound in the numerical model. Below is a graphical representation of sound pressure level in the receiver (see Fig. 6).

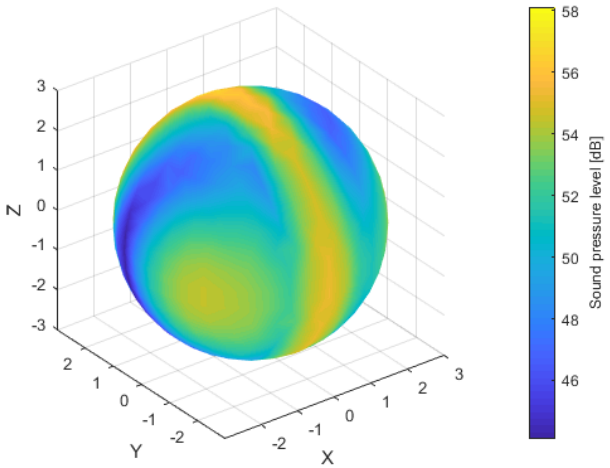

Figure 6. Distribution of the sound pressure level on 3 m radius sphere.

On the basis of the presented results, it can be seen that the highest values of the sound pressure level appear in the receivers at the height of the rotor blades. Accurate observation is that the rotating blades in the interaction with the pipeline will generate more noise than the hub, hence the results are not a surprise. The values of the sound pressure level around the rotor rotation axis ranged between 55 dB and 58 dB. An interesting fact is that the sound pressure level calculated in the rotor axis is higher on the upstream side of the rotor by a few decibels than behind it. On the downstream side it was in the range of 48 dB to 52 dB, while on the upstream side it was in the range of 50 dB to 56 dB. The higher value of the sound pressure level on the upstream side is due to the turbulent nature of the flow caused by the shape of the pipeline.

Acknowledgments

This research was supported in part by PL-Grid Infrastructure.

Additional information

The author declare: no competing financial interests and that all material taken from other sources (including their own published works) is clearly cited and that appropriate permits are obtained.

References

1. M. Konstantinov, C. Wagner; Numerical simulation of the sound generation and the sound propagation from air intakes in an aircraft cabin; New results in numerical and experimental fluid mechanics XI, Cham: Springer, 2018.
2. E. Sundström, B. Semlitsch, M. Mihăescu; Acoustic signature of flow instabilities in radial compressors; Journal of Sound and Vibration, 2018, 434, 221–236.
3. J. Al-Am, V. Clair, A. Giauque, J. Boudet, F. Gea-Aguilera; A parametric study on the les numerical setup to investigate fan/OGV broadband noise; International Journal of Turbomachinery, Propulsion and Power, 2021, 6(2), 12.
4. C. Kissner, S. Guérin, P. Seeler, M. Billson, P. Chaitanya, P. Carrasco Laraña, H. de Laborderie, B. François, K. Lefarth, D. Lewis, G. Montero Villar, T. Nodé-Langlois; Acat1 benchmark of rans-informed analytical methods for fan broadband noise prediction - part I - influence of the rans simulation; Acoustics, 2020, 2(3), 539–578.
5. F.R. Menter; Zonal Two Equation k-ω Turbulence Models for Aerodynamic Flows; AAIA Paper 93-2906, 1993.
6. Ansys Fluent: Theory Guide; Ansys Inc., 2015.
7. J. E. Ffowcs-Williams, D. L. Hawkings; Sound Generation by Turbulence and Surfaces in Arbitrary Motion; Proc. Roy. Soc. London, 1969, A264:321–342.
8. M.J. Lighthill; On Sound Generated Aerodynamically. Proc. Roy. Soc. London, 1952, A211:564-587.
9. H. Versteeg, W. Malalasekera; An Introduction to Computational Fluid Dynamics: The Finite Volume Method; Harlow, England: Pearson Education Limited, 2011.
10. H. Kumawat; Modeling and simulation of axial fan using CFD; International Journal of Mechanical, Industrial and Aerospace Sciences, 2014, 8, 11, 1892–1896. DOI:10.5281/zenodo.1337905
11. S. Fortuna; Wentylatory; Podstawy teoretyczne, zagadnienia konstrukcyjno-eksploatacyjne i zastosowanie; Kraków, Techwent, 1999.
12. J. Foss, D. Neal, M. Henner and S. Moreau; Evaluating CFD Models of Axial Fans by Comparisons with Phase-Averaged Experimental Data; Proceedings of the SAE Vehicle Thermal Management Systems Conference, Nashville, 2001, 363, 83-92.